Discrepancy quantification between experimental and simulated data of CO₂ adsorption isotherm using hierarchical Bayesian estimation

Sotaro Kojima¹, Jongwoo Park², Eli A. Carter³, Krista S. Walton³, Matthew J. Realff³, David S. Sholl^{3,4}, Tomoyuki Yajima¹, Junpei Fujiki¹, Yoshiaki Kawajiri^{1,3*}

- 1) Department of Materials Process Engineering, Nagoya University, Furo-cho 1, Chikusa, Nagoya 464-8603, Japan
- 2) National Energy Technology Laboratory, United States Department of Energy, Pittsburgh, PA 15236 USA
- 3) School of Chemical & Biomolecular Engineering, Georgia Institute of Technology, 311 Ferst Drive, Atlanta, GA 30332-0100, USA
- 4) Oak Ridge National Laboratory, Oak Ridge, TN 37830, USA

*Corresponding Author: Yoshiaki Kawajiri, Ph.D.

Tel & Fax: +81-52-789-3263 E-mail: kawajiri@nagoya-u.jp

Abstract

To quantitatively analyze the inconsistencies commonly observed between experimental and simulated adsorption isotherms, parameter estimation of adsorption isotherm models was conducted by hierarchical Bayesian estimation with parameter uncertainties being quantified as probability distributions. The estimation method was implemented using Markov Chain Monte Carlo (MCMC) to analyze multiple data sets obtained from different sources, including a publicly available database. To describe the discrepancies of experimental and simulated adsorption data, the simulation data was set as the reference to which experimental measurements were compared. We applied the proposed approach to analyze CO₂ adsorption isotherms that are measured and simulated on zeolite 13X and MIL-101(Cr). For both systems, a multiplicative factor and standard deviation of the measurement error in each data set were quantified along with a single set of the isotherm model parameters. In these case studies, the discrepancy of CO₂ adsorption isotherm was successfully quantified between experimental measurements and predictions given by molecular simulations using Grand Canonical Monte Carlo (GCMC). This approach can be a powerful tool in resolving variations among adsorption data sets obtained from different resources, as well as in providing insights into the deviations between experimental data and molecular simulations.

1. Introduction

Emission of carbon dioxide (CO₂) from fossil fuel combustion is the underlying cause of global warming. To mitigate these emissions, CO₂ capture, utilization, and storage (CCUS) is expected to be a key technology. For the practical application of CCUS, however, cost reduction especially in the CO₂ capture step is a critical challenge. Some techniques already implemented at a large scale, such as liquid amine scrubbing, have remaining challenges, including high regeneration energy, solvent evaporation, amine degradation, and equipment corrosion[1-3]. To this end, the development of alternative techniques overcoming these drawbacks, especially the high energy cost, is desired. In the past several decades, a large number of CO₂ capture techniques including advanced solvents, adsorption, and membrane separation have been studied[4]. Among them, adsorptive separation is considered one of the promising methods to recover CO₂ in flue gas from various sources[5].

For designing adsorption processes, both equilibrium and kinetic data are required, and especially obtaining reliable adsorption equilibrium data is vital[6-7]. To date, many researchers have conducted laboratory experiments and molecular simulations of CO₂ adsorption on various adsorbents, including zeolites, porous carbons, amine-modified silicas, and metal-organic-frameworks (MOFs) to identify promising materials. These efforts have generated a large amount of data on CO₂ adsorption equilibria of various materials.

To use those data effectively, open database projects such as the one by the National Institute of Standards and Technology (NIST) are ongoing, which can be useful resources for material screening and process design[8]. However, there are still some remaining challenges for practical application of these databases for material and process development. One of them is the reliability of data, namely, how to select the appropriate data from multiple data sources. Park et al.[9] reported that CO₂ adsorption measurements in MOFs obtained by different researchers show substantial variations even at well-defined adsorption conditions. Similar studies also highlighted the need for experimental reproducibility for a range of adsorbates and porous adsorbent materials [10-11]. Such variations arise for different reasons including the measurement methods (i.e., equipment, procedures, and sample conditions) as well as adsorbent degradation that may occur during material synthesis and/or post-synthesis (e.g., defects in the crystals, trace components, insufficient deactivation, and pore blockage/collapse) [12-16].

In addition to analyzing experimental data, molecular simulation is a powerful approach to predict adsorption equilibrium for adsorbents where a systematic experimental investigation can be challenging[17-19]. Nevertheless, it is unlikely the

simulated adsorption properties will exactly match those from experiments, because not all computational approximations can fully address the structural nature of adsorbents[20-21] and the molecular interactions of adsorbing species within adsorbents[22-23]. As a result, researchers face the problem of trusting simulated data over experimental data and/or vice versa, in recognition of fundamental assumptions of molecular simulation and uncertainties in experimental measurement[24].

Recently, Shih et al.[24] introduced a hierarchical Bayesian estimation method to quantify the discrepancy among experimental data sets using a Markov Chain Monte Carlo (MCMC) method. This approach can generate probability distributions for the parameters in a given adsorption isotherm model[25]. The method also gives information on multiple data sets obtained by different researchers, and hence allows the quantitative analysis of discrepancy among multiple experimental data sets.

In this study, the discrepancies of experimental data sets from a reference Grand Canonical Monte Carlo (GCMC) data are quantified by hierarchical Bayesian estimation, and parameters in isotherm models were estimated for porous adsorbents that are obtained from various sources. Among these data sets, simulated data by GCMC, which assumes adsorption occurs in defect-free crystals with interaction parameters specified by a force field, was chosen as the reference[26-28]. This choice is not intended to imply that the simulation data is the "correct" answer, but rather to note that it is typically easier to obtain high resolution data with small uncertainties using molecular simulations. Our approach is demonstrated for two case studies: zeolite 13XNa, one of the traditional and notable materials for CO₂ capture [29-37], and MIL-101(Cr), a promising MOF widely known for CO₂ adsorption[38-41].

2. Methods

2.1 Case studies: CO₂ adsorption on zeolite 13XNa and MIL-101(Cr)

2.1.1 Data collection from NIST adsorption database for zeolite 13XNa

For zeolite 13XNa, experimental CO₂ isotherm data from five different reports (hereafter labeled Exp. 1-5) were collected from the NIST adsorption database [42-46]. For computational results, GCMC simulation data from Purdue et al.[47] was used. All CO₂ isotherms used are shown in Figures S1 and S2.

The experimental conditions for each isotherm data set and zeolite sources for Exp. 1-5 as well as the simulation condition for GCMC predictions are summarized in Table S3. It is worthwhile to note that the zeolite implemented in each experiment was obtained from different supplier, and the measurement methods (i.e., apparatus and pretreatment) were also different. In each experimental data set, the measurement protocols as well as the crystal properties of 13X samples (e.g., Si/Al ratio, presence and/or absence of binders) are different, which may have led to the laboratory uncertainties in the adsorption equilibrium experiments.

It is also important to note that the GCMC simulation data used here cannot account for all possible contributions to adsorption in real samples. For example, these simulations cannot capture adsorption in non-crystalline mesopores that have been shown to make small contributions to high pressure CO₂ adsorption in reference zeolites[48].

2.1.2 Molecular simulation and isotherm measurement for MIL-101(Cr)

CO₂ adsorption data on MIL-101(Cr) are obtained by in-house GCMC prediction and experiments (Figures S3 and S4, respectively). To support the design of a post-combustion CO₂ capture process at sub-ambient conditions within a narrow CO₂ partial pressure range for this promising MOF [41,49] adsorption isotherms are simulated and measured at a sub-ambient temperature window from 223 to 273 K at an interval of 10 K in a pressure regime up to 1.0 bar.

GCMC simulation was conducted using the RASPA package [50-51]. The standard force fields of UFF[52] and TraPPE[53] are employed for Lennard-Jones parameters on MOF atoms and on quadrupolar CO₂ molecule, respectively, to determine van der Waals interactions that is defined by Lorentz-Bethelot mixing rules[54]. A long-range Ewald Coulombic interactions[55] are modeled with atomic point charges on MOF atoms and on CO₂ molecules assigned by DDEC[56-58] and TraPPE[53], respectively. To represent the crystal structure of MIL-101(Cr), as-distributed .cif file from the RASPA was adopted.

The structure of the adsorbent was assumed to be rigid in all calculations.

Two samples of MIL-101(Cr), A and B, were synthesized separately, following the general procedure outlined by Darunte et al[59]. The modulators used for Sample A and B were different; in the synthesis of Sample A, 7.5 ml of glacial acetic acid was used, while for Sample B, 7.5 ml of a 36% (v/v) solution of acetic acid in deionized water was added. The BET surface area of A was measured to be 2760 m²/g. More details of material synthesis, isotherm and surface area measurements are given in the supplementary material.

2.2 Adsorption equilibrium models

There are various mathematical models to represent adsorption isotherms such as Langmuir, Freundlich, Henry, BET, Sips, and Toth models [60-61]. To select an appropriate isotherm model for accurate prediction, various model selection criteria based on error evaluation including square of correlation coefficient (R²), adjusted R² (adj- R²), sum of the squares of errors (SSE), root mean square deviation (RMSD), and hybrid fractional error function (HYBRID) are frequently used [62]. However, these criteria, with the exception of adj-R², do not take into account the number of parameters in the functional forms. Recently, information-based criteria such as Akaike information criterion (AIC), Bayesian information criterion (BIC), and their extensions have been applied for selecting the best isotherm model among the candidates having the different number of parameters[63-65]. Below, AIC and BIC were employed for selecting the most suitable adsorption isotherm model, where lower values of AIC and BIC indicate a better model.

It is known that CO₂ adsorption isotherms on zeolite 13X can be described well either by the Toth model [66-67] or the dual-site Langmuir model [68-70]. Several candidate models with different number of parameters were investigated for the GCMC data (see Table S1 in the supplementary material). By comparing the values of AIC and BIC, the Toth model with the temperature dependence of the parameter *t* given in Eqs. 1-3 (model 3 in Table S1)[71] was eventually employed for the equilibrium model of CO₂ adsorption on zeolite 13X:

$$q^* = q_s \frac{b_T p}{(1 + (b_T p)^t)^{1/t}} \tag{1}$$

$$b_T = b_{T0} \exp\left(\frac{-\Delta H}{RT}\right) \tag{2}$$

$$t = A_t + \frac{B_t}{T} \tag{3}$$

where q^* is the equilibrium amount of CO₂ adsorbed; q_s is the saturated amount of CO₂ adsorbed at a given temperature T; b_T is the affinity constant; t is the Toth constant representing the heterogeneity of adsorption system; p is the partial pressure of CO₂; b_{T0} is the preexponential factor for the affinity constant; ΔH is the isosteric heat of adsorption; R is the ideal gas constant; A_t and B_t are temperature dependence constant of parameter t.

For MIL-101(Cr), on the other hand, the Sips model as given in Eqs. 4-5 (model 7 in Table S2), was chosen over the Langmuir and Toth models:

$$q^* = q_s \frac{(b_s p)^{1/n}}{1 + (b_s p)^{1/n}} \tag{4}$$

$$b_S = b_{S0} \exp\left(\frac{-\Delta H}{RT}\right) \tag{5}$$

where b_S is the affinity constant; n is the Sips constant; and b_{S0} is the preexponential factor for affinity constant. Using the two model selection criteria, AIC and BIC, the Sips model shows the minimum values as summarized in Table S2.

2.3 Hierarchical Bayesian model

The Bayesian approach to describe parameter uncertainty is a method for estimating parameter values with probability distributions following the Bayes' theorem [25]. The principle of Bayesian estimation is given by:

$$p(\mathbf{\Theta}|\mathbf{y}) = \frac{p(\mathbf{y}|\mathbf{\Theta})p(\mathbf{\Theta})}{p(\mathbf{y})} \propto p(\mathbf{y}|\mathbf{\Theta})p(\mathbf{\Theta})$$
(6)

where Θ is the parameter vector to be estimated; y is the vector of data such as experimental or simulated data; $p(\Theta)$ is the prior probability distribution of Θ ; $p(y|\Theta)$ is the likelihood representing the probability of data y at a given parameter Θ ; and p(y) is called the marginal likelihood that normalizes $p(y|\Theta)p(\Theta)$. The above equation shows that normalization by p(y) is needed to obtain the posterior distribution of the parameters.

In Bayesian estimation, the posterior probability distribution can be obtained by updating the prior probability distribution using MCMC sampling. Hence a large enough

number of samples are required for obtaining the posterior distributions of the parameters. Estimating parameters as a probability distribution, in comparison to the point estimation such as the least squares method, gives us the information on the parameter uncertainty. In addition, correlations among parameters can be found by analyzing the samples obtained by MCMC [72].

Generally, it is difficult to determine a parameter Θ by a conventional Bayesian estimation approach when data sets y are obtained under different conditions; that is, a single set of probability distributions for Θ cannot be easily obtained for a variety of CO_2 adsorption data that are measured at different experimental conditions and/or obtained by distinct methods (either experiment or simulation). Ignoring the differences in the condition of each data set would lead to *overdispersion* of the parameter Θ , where the variation of Θ is estimated to be large. To overcome this problem of finding a single parameter set from different data sources, hierarchical Bayesian inference is an well-known approach in Bayesian statistics[73] which can be applied to analyze adsorption isotherms as demonstrated earlier by Shih et al.[24]. Below, we employ this approach for the first time to quantify the discrepancy of isotherm data measured in laboratory from those predicted by molecular simulation.

The principle of hierarchical Bayesian estimation is given by the following joint prior distribution [25]:

$$p(\boldsymbol{\theta}, \boldsymbol{\omega}, \boldsymbol{\varphi}) = p(\boldsymbol{\theta})p(\boldsymbol{\omega}|\boldsymbol{\varphi})p(\boldsymbol{\varphi}) \tag{7}$$

where θ is a vector of *common parameters* in the model, ω is an *individual parameter* for each data set, and φ is a hyperparameter. This equation expresses $p(\theta, \omega, \varphi)$ using a conditional probability distribution $p(\omega|\varphi)$ and the probability $p(\varphi)$, assuming θ is independent of ω . In this model, the heterogeneity in each data set is considered by introducing an additional individual parameter ω for each data set to describe unique properties in each data set such as experimental conditions. The dispersion of parameter ω is represented by hyperparameter φ which is an unknown variable having its own prior distribution. Redefining Θ in Eq. 6 as $\Theta = (\theta, \omega, \varphi)$ followed by combining Eqs. 6 and 7 gives the framework of the hierarchical Bayes estimation as:

$$p(\theta, \omega, \varphi | y) \propto p(y | \theta, \omega, \varphi) p(\theta, \omega, \varphi) = p(y | \theta, \omega) p(\theta, \omega, \varphi) = p(y | \theta, \omega) p(\theta) p(\omega | \varphi) p(\varphi)$$
(8)

where $p(\theta, \omega, \varphi | y)$ is the posterior distribution; $p(y | \theta, \omega)$ is the likelihood calculated from

the isotherm model; $p(\varphi)$ is the hyperprior distribution to quantify prior knowledge about the prior distribution $p(\varphi|\omega)$. In the above equation, we assume $p(y|\theta,\omega,\varphi) = p(y|\theta,\omega)$; i.e. y is conditionally independent of φ given θ and ω .

2.4 Parameter estimation by hierarchical Bayesian model

Based on the hierarchical Bayesian framework, we attempt to obtain a single set of parameters in the isotherm model and quantify the uncertainties of adsorption equilibrium data which are measured and predicted by different group of researchers. To do so, the discrepancy must be modeled carefully to account for possible contributors to the variations or errors in data sets from different research groups. For experimentally measured data, the pre- and post-synthesis procedures such as activation, degradation or aging, and the presence of non-adsorbing defect sites in the adsorbents among many others [9,74] can be the contributors. For data from molecular simulations, the absence of defects and/or deformations in the simulated material and the imprecision of the force fields used to define adsorbate/adsorbent interactions will contribute to variations with respect to experimental data.

In general, the relationship between the data y_i , where i is the index of each data set, and the model y^* is linked with the *additive* error ε_i as follows:

$$y_i = y^* + \varepsilon_i, \ \varepsilon_i \sim N(0, \sigma_i^2)$$
 (9)

In this equation, the additive error ε_i of each data is modeled using an individual parameter σ_i . This parameter σ_i is the standard deviation (SD) of vector \mathbf{y}_i representing the unique model error of each data set such as measurement noise. However, ε_i alone would not fully address the uncertainty contributors in the measured amounts of adsorption discussed above. Some uncertainty contributors, such as defects and impurities in the crystals, would not be modeled only by additive errors.

In addition to ε_i , a *multiplicative* factor R_i is introduced to complementarily lump potential uncertainty contributors. This parameter R_i represents the multiplicative error in the adsorption amounts between each data set y_i (= q_i^{eq}) and model y^* (= q^*). The equation that takes into account both the multiplicative and additive errors can now be written as:

$$q_i^{eq} = q^* \cdot R_i + \varepsilon_i , \ \varepsilon_i \sim N(0, \sigma_i^2)$$
(10)

where q^* is amount of CO₂ adsorbed at equilibrium defined by Eqs. 1-3 or Eqs. 4-5.

Despite the fundamental limitations that exist in molecular modeling of gas adsorption, such as assigning the atomic point charges and choosing the force fields [17-19], GCMC data can serve as a *reference* in uncertainty quantification as they assume an ideal condition that minimizes the external variation contributors on adsorption data as discussed above for experiments. We therefore set $R_{GCMC} = 1$, while allowing the additive error ε_{GCMC} to take non-zero values. The concept of the parameter R_i is illustrated in Figure 1, showing this parameter plays a vital role in addressing deviations between measurements and GCMC predictions.

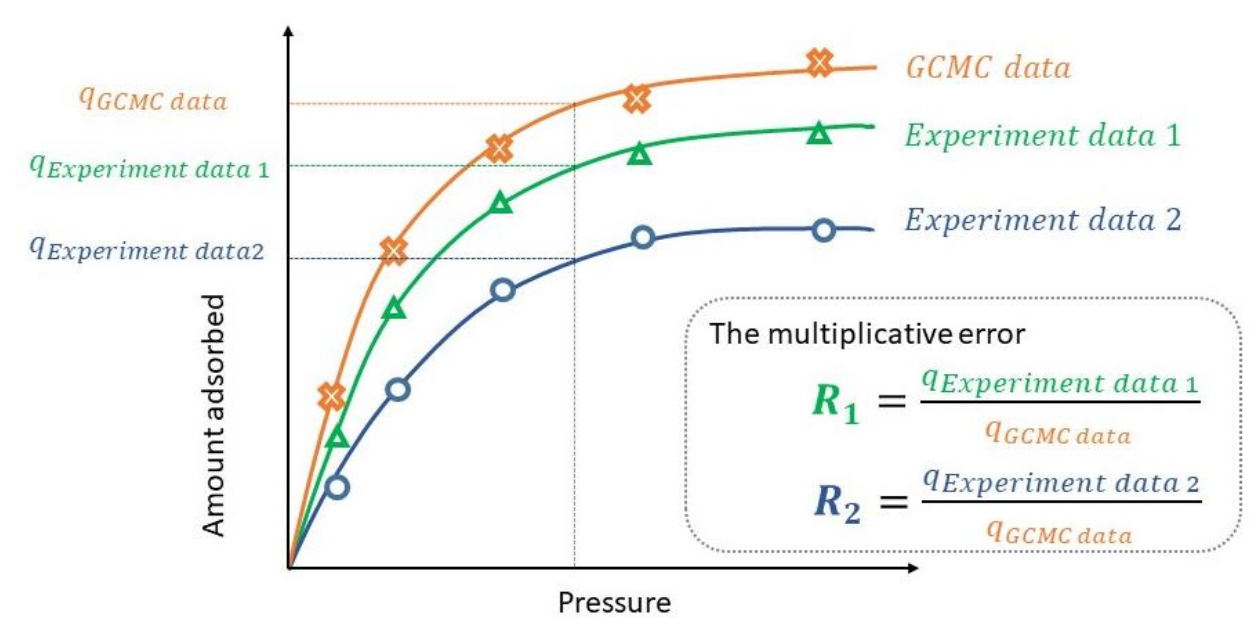


Figure 1 Illustration of the hierarchical Bayesian estimation for adsorption isotherm data using multiplicative factor R_i .

Using Eq. (10), the individual parameters $\omega_i = (R_i, \sigma_i)$ in Eq. (8) were estimated for each data set applying the common parameter vector $\boldsymbol{\theta}$ on the chosen adsorption isotherm models. The prior distributions of the hyperparameter $\boldsymbol{\varphi}$ are uniform with the upper and lower bounds parameterized as $\boldsymbol{\varphi} = (\{R^{\text{lower}}, R^{\text{upper}}\}, \{\sigma^{\text{lower}}, \sigma^{\text{upper}}\})$. The structure of the hierarchical Bayesian model used in this study is illustrated in Figure 2.

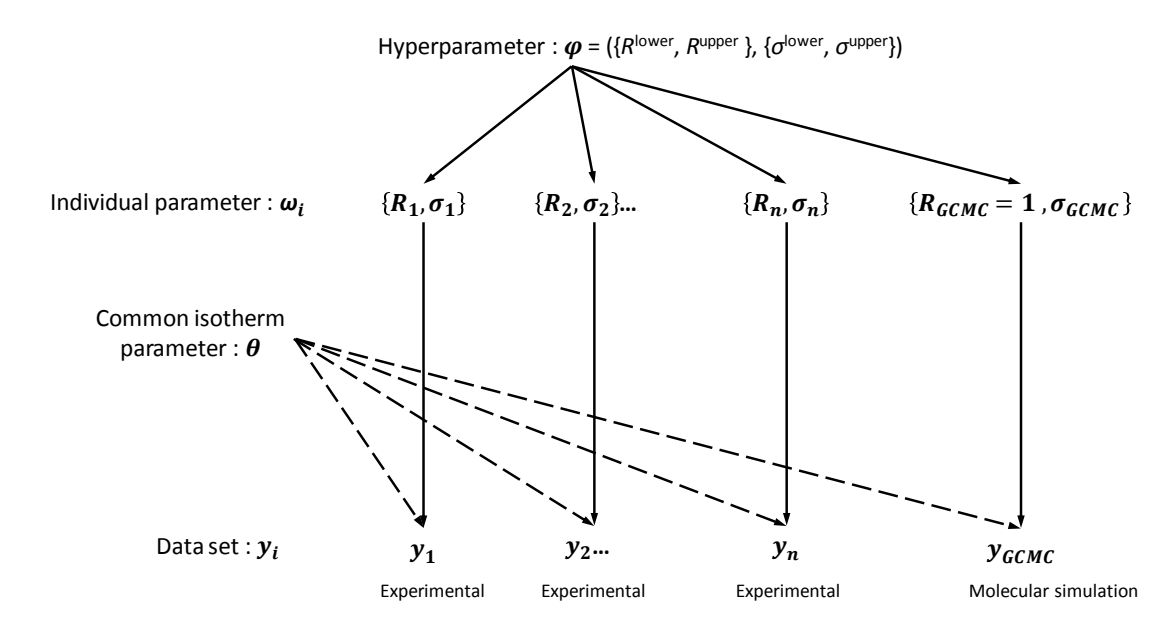


Figure 2 Structure of the hierarchical Bayesian model applied in this study.

2.5 Prior distributions and conditions for MCMC analysis

It is difficult to solve p(y) in Eq. 8 analytically. In this study, the MCMC method was used to solve this equation approximately. The analysis conditions for the MCMC are listed in Table 1. The posterior distribution of the parameters was determined from the last 5,000 MCMC sampling points with a thinning interval of 50 and burn-in of 1,000,000. As a confirmation of the convergence of the obtained posterior distributions, the autocorrelation and trace plots were checked.

In Bayesian estimation, it is necessary to provide an appropriate prior distribution for each parameter and hyperparameter. Prior knowledge about parameters and hyperparameters (e.g., experts' knowledge, previous studies, etc.) should be incorporated into the prior distribution. Some trial-and-error attempts to find reasonable prior distributions are often performed to assure convergence. A typical choice of prior distributions is uniform distributions over a sufficiently wide range (non-informative prior). For example, the prior distribution for the parameter σ_i , which represents the measurement error for each data set i, was determined to be sufficiently wide. We checked the sensitivity of the width to the posterior distributions to assure robustness of the estimation. On the other hand, if there is a strong *belief* that a parameter must be within a specified range, narrow prior distributions can be chosen. For instance, the parameter R_i , which represents the multiplicative factor, is expected to be around 1. This is our belief that experimental and simulated data should match reasonably well.

The estimation conditions for the prior distribution of parameters in adsorption isotherm models and the hyperparameters on zeolite 13X and MIL-101(Cr) are listed in Table 2(a) and 2(b), respectively. As discussed later, the isotherm parameter vector is given by $\theta = (b_0, -\Delta H, q_s, A_t, B_t)$ for zeolite 13X, and $\theta = (b_0, -\Delta H, q_s, n)$ for MIL-101(Cr). Uniform distributions with upper and lower bounds that are sufficiently wide were employed for all parameters and hyperparameters in both systems, except for the heat of adsorption $-\Delta H$ and saturated capacity q_s for zeolite 13X. For $-\Delta H$ for zeolite 13X, a normal distribution was used as the prior distribution based on the experimentally measured value of 38.63 kJ/mol from the literature [75]. This value was taken as the mean, and SD of 5.10 kJ/mol was employed which includes the range of $-\Delta H$ between 28.63 and 48.63 kJ/mol at the probability of 95%. The prior distribution of the parameter q_s was found by visual inspection (see Figure S2(b)).

Table 1 Analysis conditions for MCMC method.

Programming language	Python3.6
MCMC method library	PyMC2
Burn-in	1,000,000
Thinning interval	50

Table 2 Prior distributions for parameters in isotherm models and hyperparameters.

(a) zeolite 13X.

Parameters		Mean	SD
<i>–∆H</i> [kJ/mol]		38.63	5.10
Parameters		Lower bound	Upper bound
b_0 [bar ⁻¹]		0.001×10^{-3}	1.0×10^{-3}
q_s [mol/kg]		0.001	20.0
A_t [-]		0.001	0.5
B_t [-]		0.001	35
Hyperparameters		Lower bound	Upper bound
R_i [-]	$R^{ m lower}$	0.001	1.000
	R^{upper}	1.000	2.000
σ_i [mol/kg]	$\sigma^{ m lower}$	0.001	0.500
	$\sigma^{ m upper}$	0.500	1.000

(b) MIL-101(Cr).

Parameters		Lower bound	Upper bound
b_0 [bar ⁻¹]		0.001×10^{-3}	1.0×10^{-3}
$-\Delta H$ [kJ/mol]		0.001	50.0
q_s [mol/kg]		40.0	80.0
n [-]		0.001	3.00
Hyperparameters		Lower bound	Upper bound
R _i [-]	$R^{ m lower}$	0.001	1.000
	R^{upper}	1.000	2.000
σ_i [mol/kg]	$\sigma^{ m lower}$	0.001	0.500
	$\sigma^{ m upper}$	0.500	1.000

3. Results and discussion

3.1 CO₂ adsorption on zeolite 13X

In our preliminary model selection, the Toth model (model 3 in Table S1) was chosen for the GCMC data (Figure S1). However, we note that the model deviates from the GCMC data to some extent, especially within the low pressure region. A similar issue of mismatch at low pressure regions is reported in literature[75]. It was also found that fitting the model becomes more challenging when multiple experimental data sets were included in addition to the GCMC data.

The CO₂ isotherms fit to zeolite 13X adsorption data were analyzed by the hierarchical Bayesian method. The parameter estimation results are shown in Figures 3 and 4. The 95% highest posterior density (HPD) and mean values of each adsorption isotherm equation parameter and hyperparameter are listed in Table S4.

As shown in Figure 3, the posterior distributions of all parameters in the isotherm equation are all nearly unimodal, despite unform distributions set as prior distributions for b_0 , q_s , A_t , and B_t . This suggests the data provide sufficient information to transform the uniform prior distributions into the unimodal posterior distributions by Bayesian principle in Eq. (8). The posterior distribution of the heat of adsorption $-\Delta H$ converged to around 28.0 kJ/mol, which is smaller than the mean of the prior distribution that we set (38.63 kJ/mol) according to literature[75]. For the equilibrium adsorption capacity q_s , the mean value of the posterior distribution (16.04 mol/kg) is much larger than the experimental adsorption capacities in the range of measured pressures. The posterior distributions of A_t and B_t also resulted in unimodal distributions that converge to non-zero

values. This confirms the importance of incorporating the temperature dependence of the Toth parameter t into the Toth model (see Eq. 3) for modeling CO_2 adsorption on zeolite 13X.

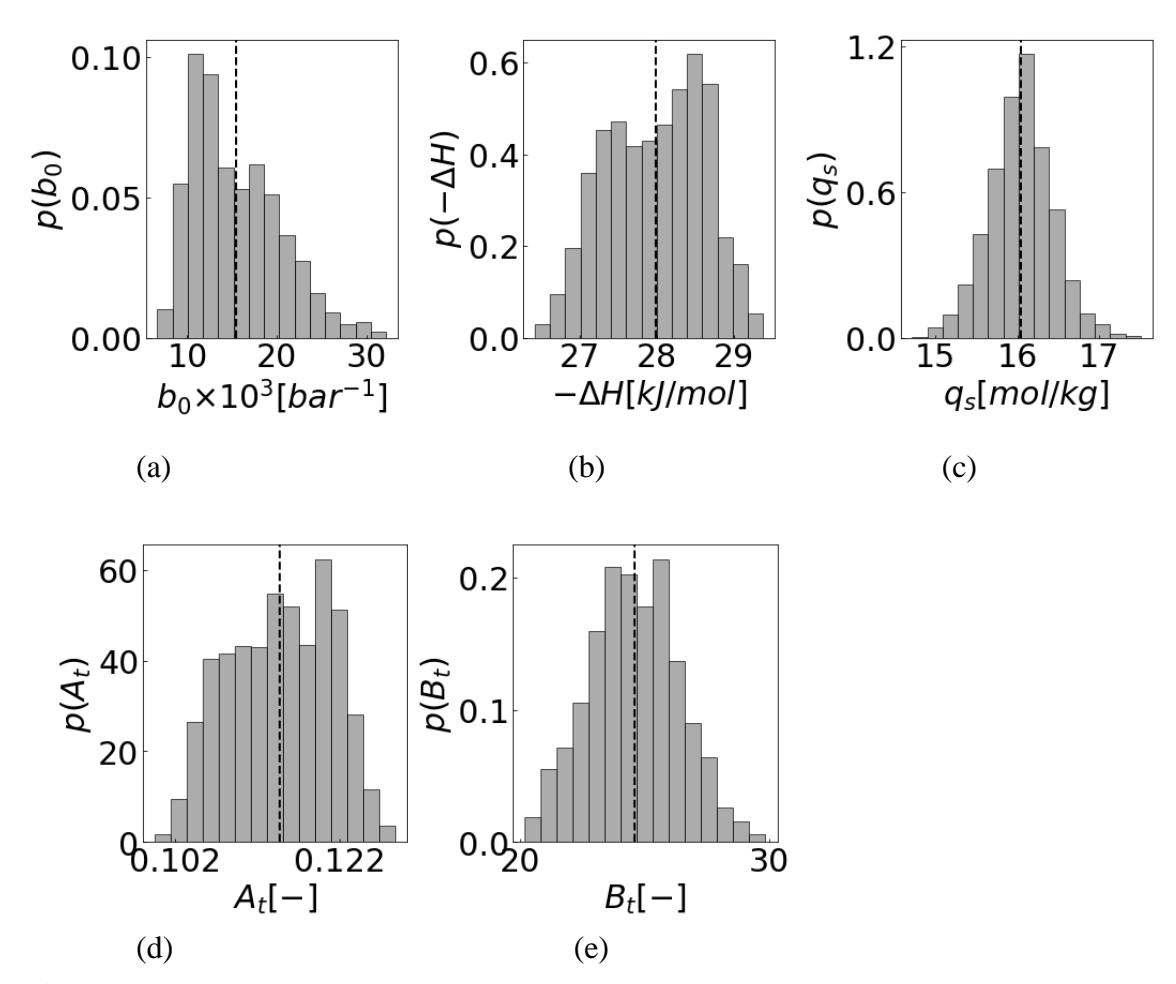


Figure 3 Posterior distributions of the adsorption isotherm equation parameter $\theta = (b_0(a), -\Delta H(b), q_s(c), A_t(d), B_t(e))$ for zeolite 13X. Vertical lines represent the mean of each posterior distribution.

The hyperparameter R_i that is used to describe the discrepancy of measurement data from GCMC resulted in posterior distributions which are unimodal and almost symmetric. It can be seen clearly in Figure 4(a) that the posterior distributions of R_3 and R_5 converged near to R_{GCMC} , indicating that Exp. 3 and 5 are in close agreement with the ideal CO₂ adsorption assumed in the GCMC simulation. For Exp. 2, on the other hand, the mean value of R_2 , 0.238, was significantly smaller than other R_i as well as than R_{GCMC} . Considering that the measurement in Exp. 2 was taken at the pressure and temperature ranges similar to those performed in the GCMC simulation, such data may be labeled as

outliers that deviate significantly from other data sets[9].

While the inconsistencies across each isotherm data set were quantified successfully by R_i , we should note that the underlying causes for the deviations between the GCMC simulation and experimental data cannot be identified relying only on this approach. Information on synthesis, preparation and measurement of the material used in each data set was limited (Table S3 in supplementary material) to conduct further analysis. To identify the reasons for the deviations, a larger amount of data sets and more information on the synthesis and measurement protocols would be needed.

Figure 4(b) shows the posterior distribution for σ_i that represents the variance of the measurements in each data set. A small value of σ_i implies narrow scatter of data from the true value, which is assumed to follow the isotherm model (Eq. 10). We find σ_3 for Exp. 3 is the smallest, and σ_4 for Exp. 4 is the largest. Our findings revisit the hurdles of high-pressure gas adsorption measurements[76-77] that lead to a larger deviation of adsorption capacities; that is, Exp. 4 was conducted for the widest pressure window whereas Exp. 3 was carried out in a narrow pressure window (Figure S2), which provide a simple implication for the values of σ_4 and σ_3 discussed above. As an aside, σ_{GCMC} is found to be large owing to a relatively poor fit to isotherm model (Figure S1).

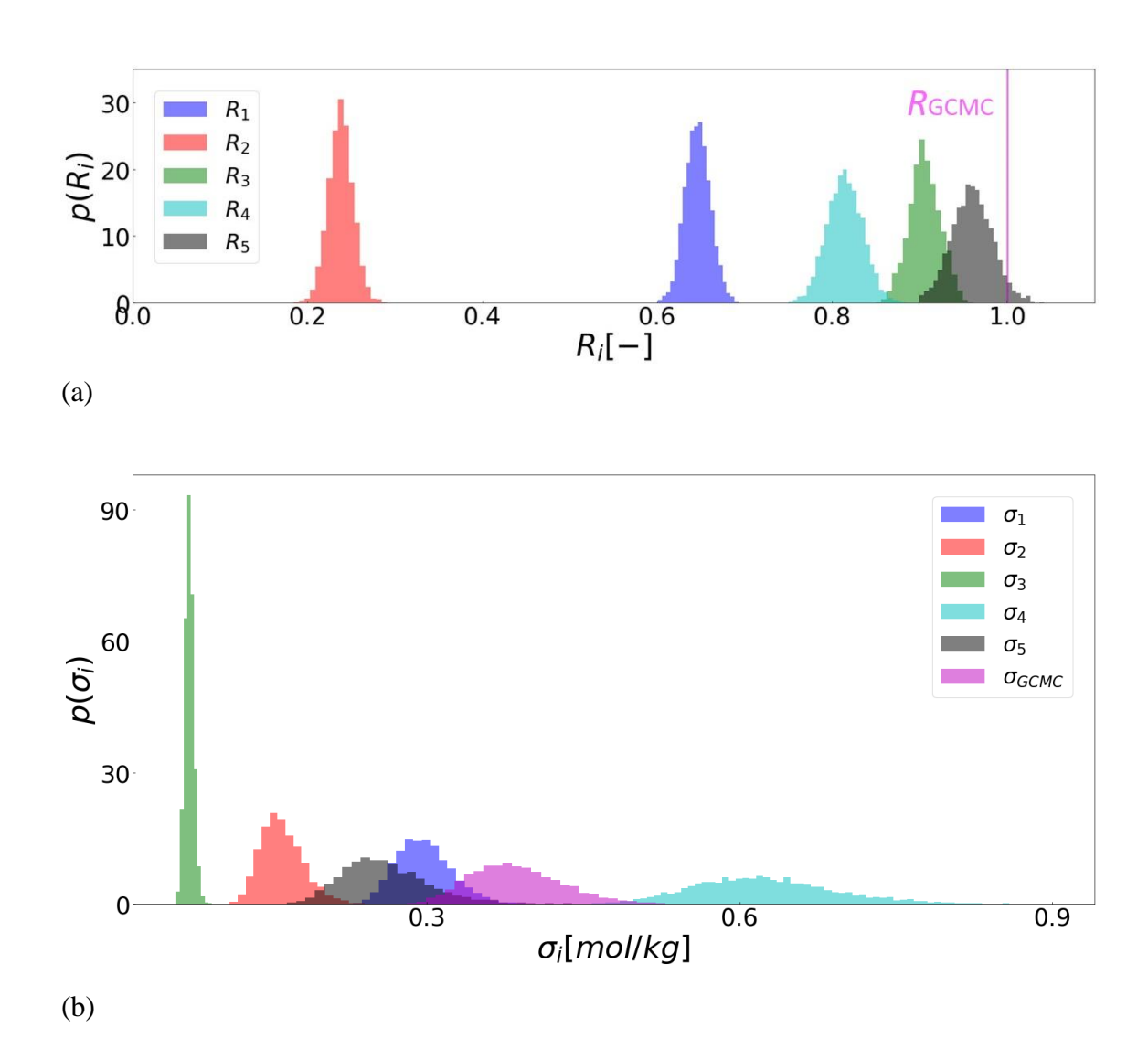


Figure 4 Posterior distributions for parameters R_i (a) and σ_i (b) for zeolite 13X.

In Figure 5, the model fitting lines are drawn by sampling isotherm parameters θ from the posterior distributions, plotted along with each experimental or simulated data set. As expected from above analysis on hyperparameters, Exp. 3 (Figure 5(c)) shows very narrow bounds of the lines (small variance of R_3) and good agreement with the model (small value of σ_3). It is noteworthy that R_i effectively quantifies the discrepancy between measured and simulated data regardless of the disparate temperature ranges that cannot be simply compared to each other[9,24]. Analysis of this kind could facilitate better measurement protocols and computational methods for gas adsorption applications [78]. In Figure 5(f), some deviation of the model from the GCMC data can be seen; while the fitting is not "perfect", the GCMC data was utilized as a reference for the experimental data in Figures 5 (a)-(e) to identify an isotherm model with a common set of parameters,

as shown in Figure 3.

Parameter accuracy and precision can be worsened by strong correlation among parameters. To analyze parameter correlations, Figure 6 shows pair plots of the parameters sampled via the MCMC algorithm. There, a sample distribution forming a circle-like shape means a weak correlation, whereas a thin ellipse-like shape indicates a strong correlation between two parameters. The parameter q_s is not likely to be correlated with any other parameters. On the other hand, we observe strong correlations between other pairs of parameters. For example, there are positive correlations for $-\Delta H$ vs. A_t and b_0 vs. B_t . Negative correlations can also be found for b_0 vs. $-\Delta H$, b_0 vs. A_t , $-\Delta H$ vs. B_t , and A_t vs. B_t . All of these correlated parameters are for describing the temperature dependence of adsorbed amounts (Eqs. 2 and 3). This suggests that more data measured or simulated at a wider range of temperatures may improve the accuracy and precision of the parameter estimation.

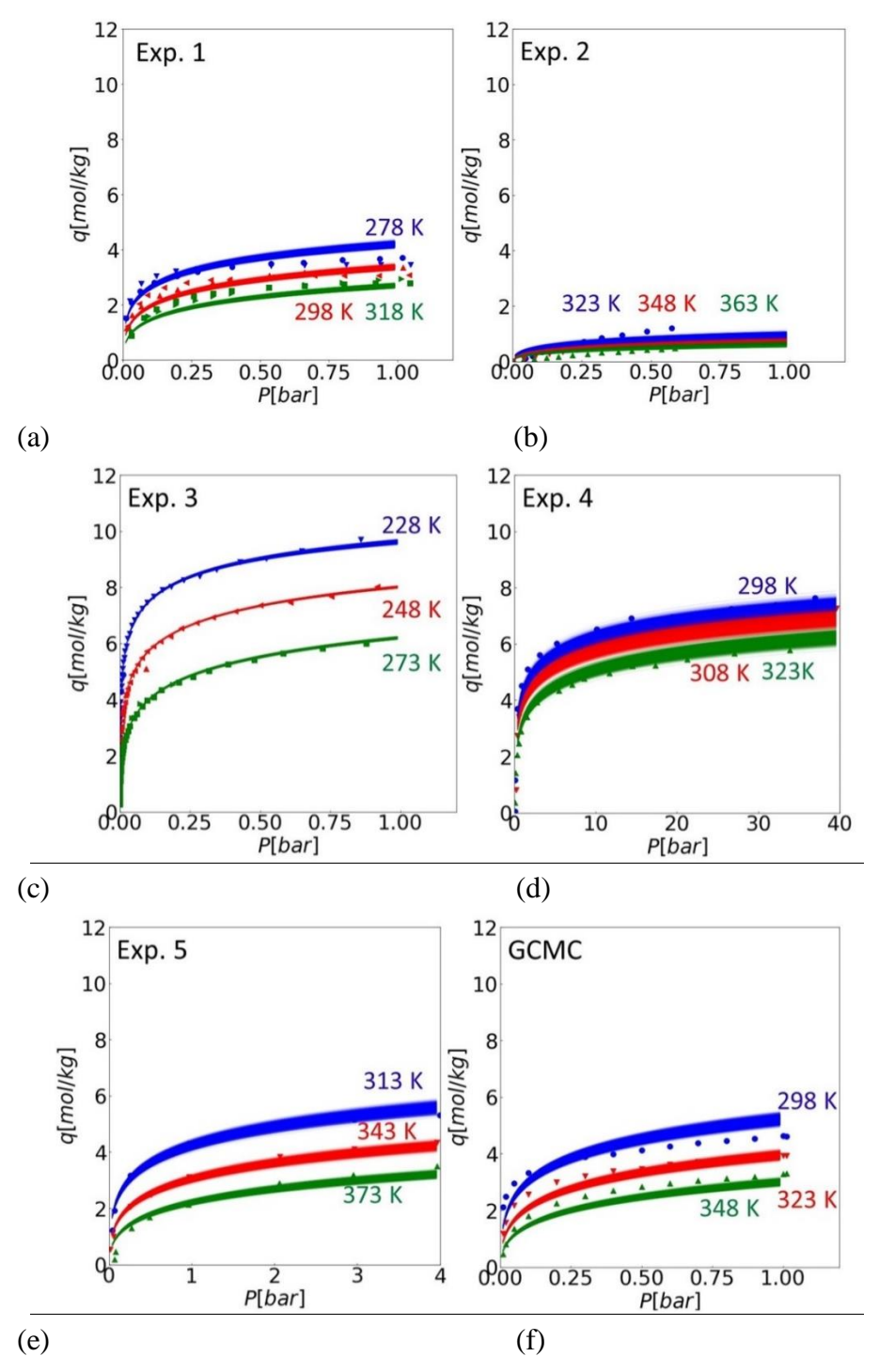


Figure 5 Data sets and the model plots using estimated isotherm parameters for zeolite 13X: (a) Exp. 1, (b) Exp. 2, (c) Exp. 3, (d) Exp. 4, (e) Exp. 5, and (f) GCMC. The model plots are shown as lines using 5,000 points sampled from parameter posterior distributions.

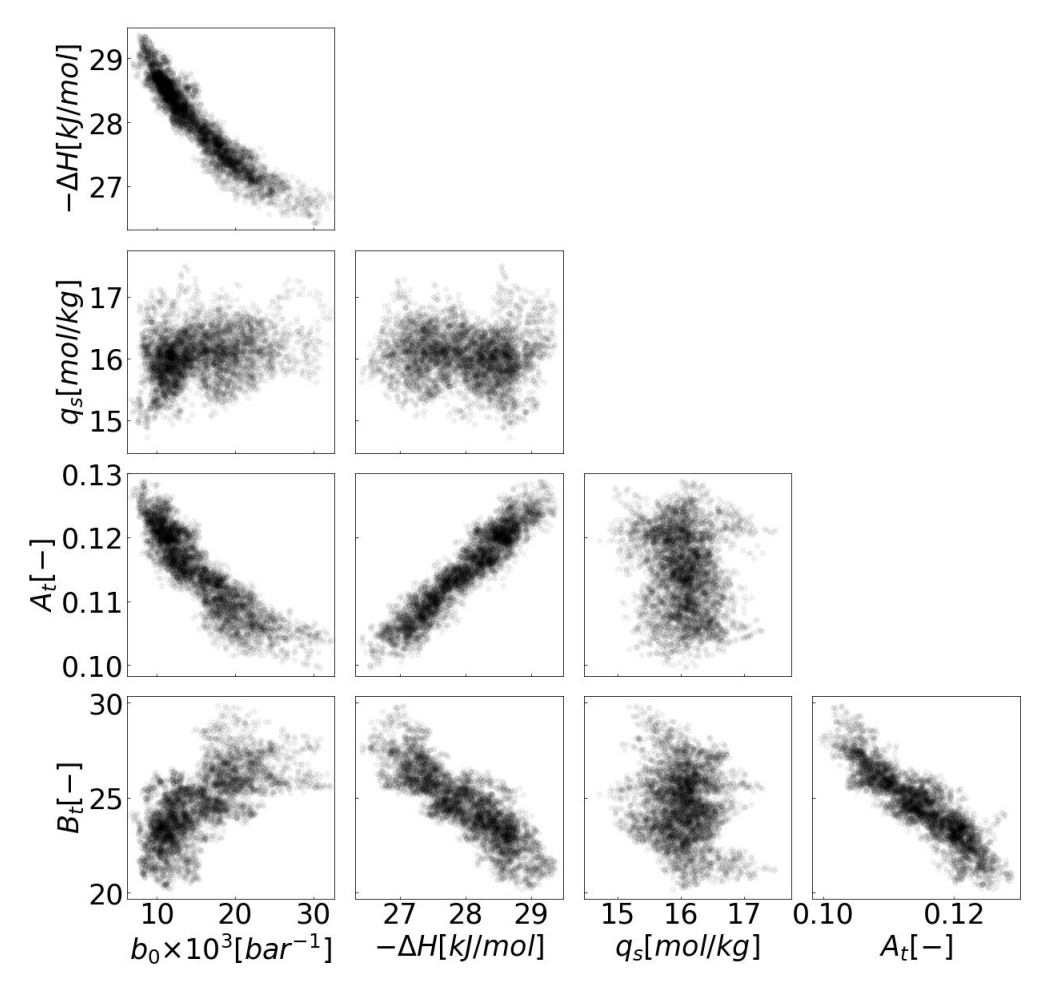


Figure 6 Parameter pair plots of adsorption isotherm model for zeolite 13X. In each pair plot, 5,000 points are sampled from parameter posterior distributions.

3.2 CO₂ adsorption on MIL-101(Cr)

Using the same hierarchical Bayesian framework, the discrepancy between experimental and simulated CO₂ isotherms was analyzed in another case study of MIL-101(Cr). The Sips model, which gives the lowest values of AIC and BIC, was employed for this system (Figure S3 in supplementary material). The isotherm parameter and hyperparameter estimation results are shown through Figures 7-9 with their mean and 95% HPD interval information given in Table S5.

Figure 7 shows the parameter estimation for the Sips isotherm model. Three of the four parameters, b_0 , $-\Delta H$, and n, exhibit unimodal posterior distributions which are nearly symmetric. On the other hand, q_s shows an asymmetric distribution with the mode reaching the upper limit of the prior distribution, which may indicate the true mean lies above the upper limit of the prior distribution and could not be found in the range of the

prior distribution; the prior distribution of this parameter was set to a uniform distribution ranging from 40 to 80 mol/kg, determined by visually examining the saturation CO₂ uptake in MIL-101(Cr) at corresponding sub-ambient temperatures (Figure S3(a)). We attempted setting the prior distribution to those with larger means, but such attempts lead to similar distributions.

The ill-shaped posterior distribution of q_s may be due to inadequacy of the isotherm model. Approximate saturation capacity of adsorbing molecules depends on the density of adsorbed phase of species within the pores. The density of CO_2 (and hence its adsorption capacity) increases as lowering temperature, where such trend becomes drastic as the temperature decreases to sub-ambient conditions [49,79]. This effect, which is not represented by the isotherm model we employed (model 7 in Table S2), may be even more significant in our sub-ambient temperature window resulting in biased q_s towards large values. Unfortunately, the relatively small amount of the data in this study did not allow us to find a better isotherm model, since employing a more complex model with a larger number of parameters (e.g. model 8 in Table S2), even with fully using the GCMC data up to higher pressure, did not lead to better posterior distribution of q_s . Obtaining additional experimental or computational data sets that cover a wider range of temperatures, for example at room-temperature, may help to overcome this challenge.

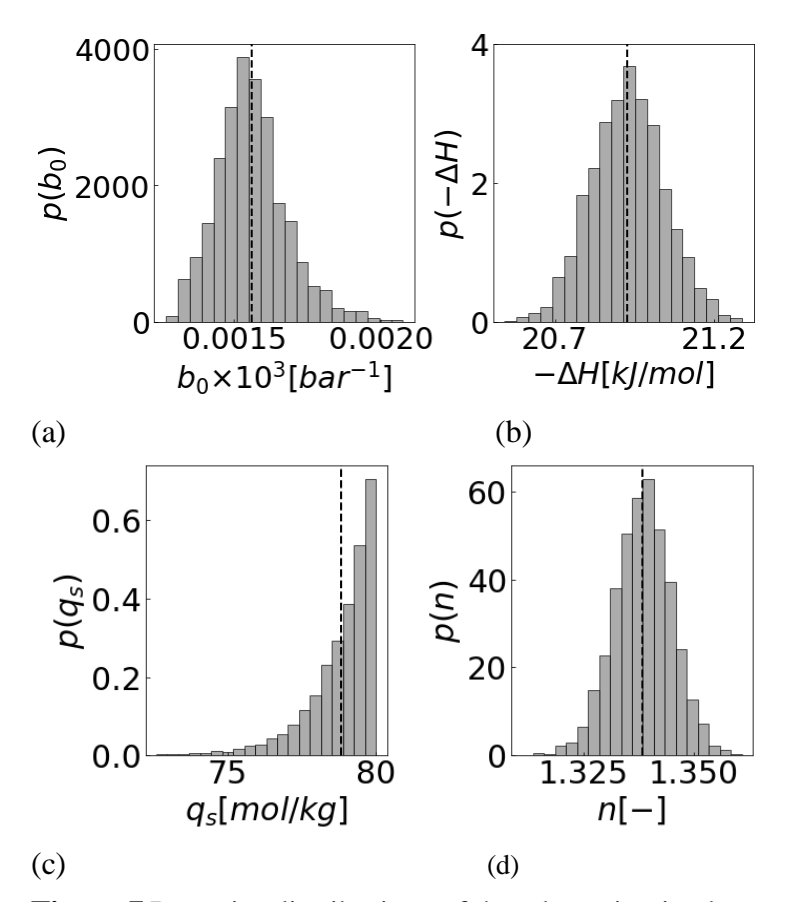
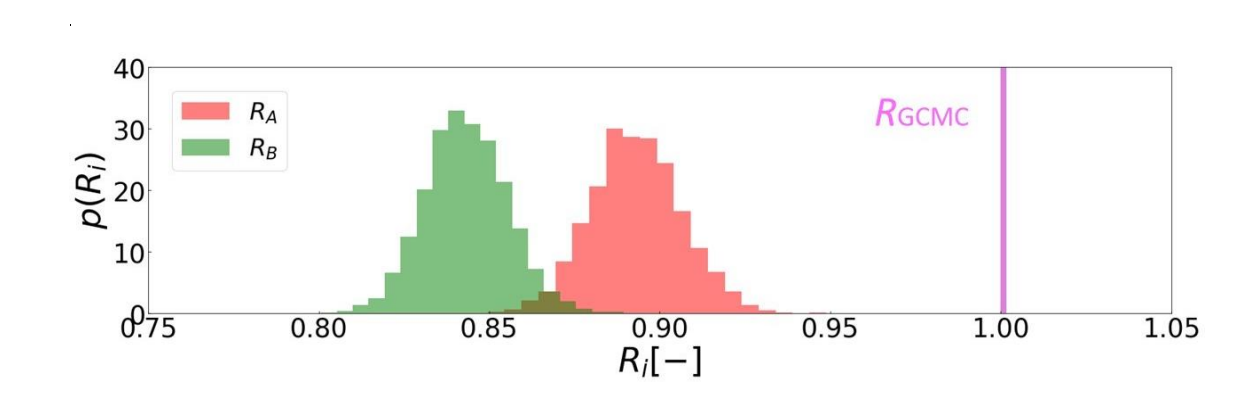


Figure 7 Posterior distributions of the adsorption isotherm equation parameter $\theta = (b_{\theta}(a), -\Delta H(b), q_s(c), n(d))$ for MIL-101(Cr). Vertical lines represent the mean of each posterior distribution.

Figure 8 shows the posterior distributions of the hyperparameters R_i and σ_i . The modes are around $R_A = 0.86$ and $R_B = 0.82$ for Exp. A and Exp. B, respectively. Figure 8(a) statistically quantifies the difference of the two experiments, where the overlapped area between $p(R_A)$ and $p(R_B)$ is only approximately 6%, owing to the sharp distributions. This small percentage of the overlapped area indicates that the two experiments, A and B, can be distinguished statistically. The values of R_A and R_B are both slightly smaller than 1, indicating the adsorbed amounts in experiments are smaller than that predicted by GCMC. These relatively minor discrepancies between experiments and GCMC can be partly explained by the difference in the surface area; the BET surface area measured experimentally for A was about 2760 m²/g, which is approximately 0.88 times the computed surface area, 3134.3 m²/g. The difference of the surface area implies non-adsorbing sites such as defects in the synthesized crystals, while GCMC assumes defect-free crystal structures which provide an ideal surface area accessible by gas molecules. In some past studies, the ratio of the measured surface area to the computed one is used

as a scaling factor [80-82]. Our approach of using R_i takes into account the difference not only in the surface area, but also other nonidealities such as measurement errors. For the posterior distribution of σ_i shown in Figure 8(b), narrow probability distributions are found for σ_A and σ_B compared to σ_{GCMC} . The relatively large value of σ_{GCMC} is due to the slight mismatch of the Sips isotherm model. Nonetheless, as examined in the previous case study of zeolite, we note σ_{GCMC} is in an acceptable range that has a marginal impact on reliable prediction of another hyperparameter R_i .

The model fit lines over actual data set are shown in Figure 9. The estimated model fits well with Exp. A and B within a narrow bound around the experimental data. On the other hand, for GCMC, slight mismatch to the simulated data can be found due to the minor disagreement between experimental and GCMC data. Such disagreement, especially in low-pressure regimes, could be resolved by tuning the GCMC details such as imposing different interatomic force fields [83-85] and adopting different atomic point charge assignment methods and determining trial move types for adsorbates with distinct probabilities. The relatively poor fit of the Sips model to GCMC may also be resolved by employing a more complex isotherm model that includes a larger number of parameters than models 1, 6, 7, or 8 in Table S2 in the supplementary material, which would require a larger amount of data.



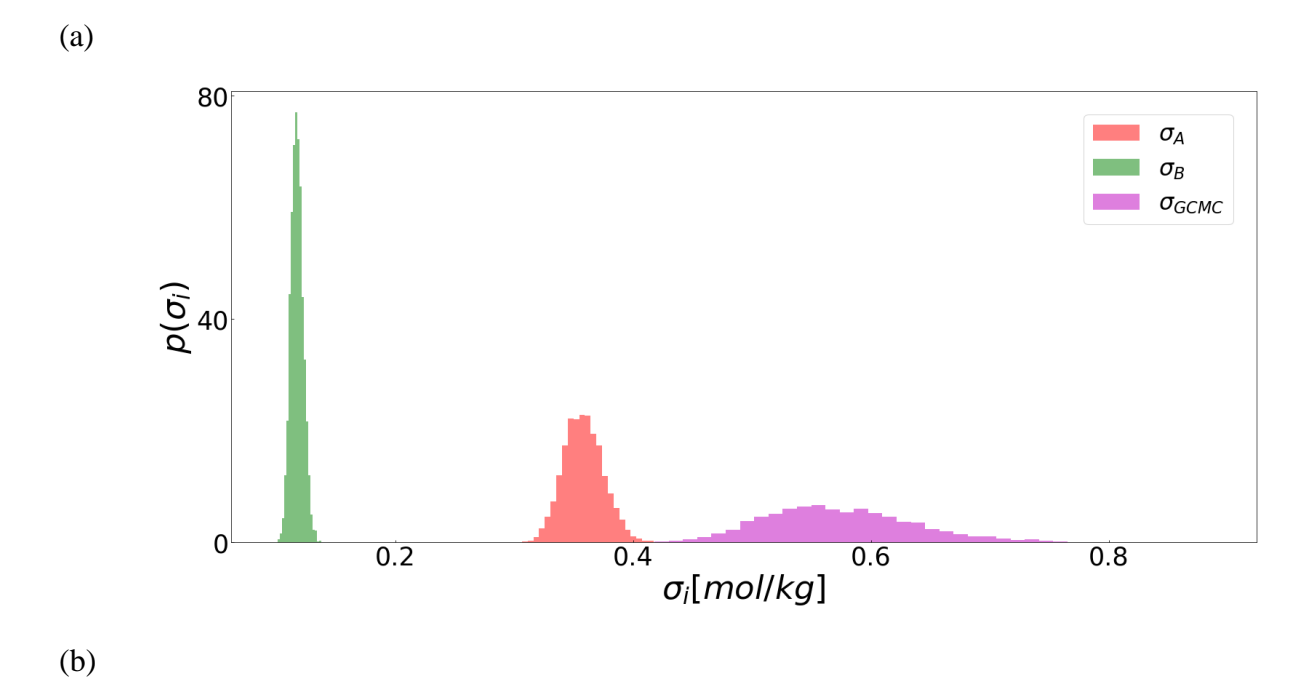


Figure 8 Posterior distributions of hyperparameters R_i (a) and σ_i (b) for MIL-101(Cr).

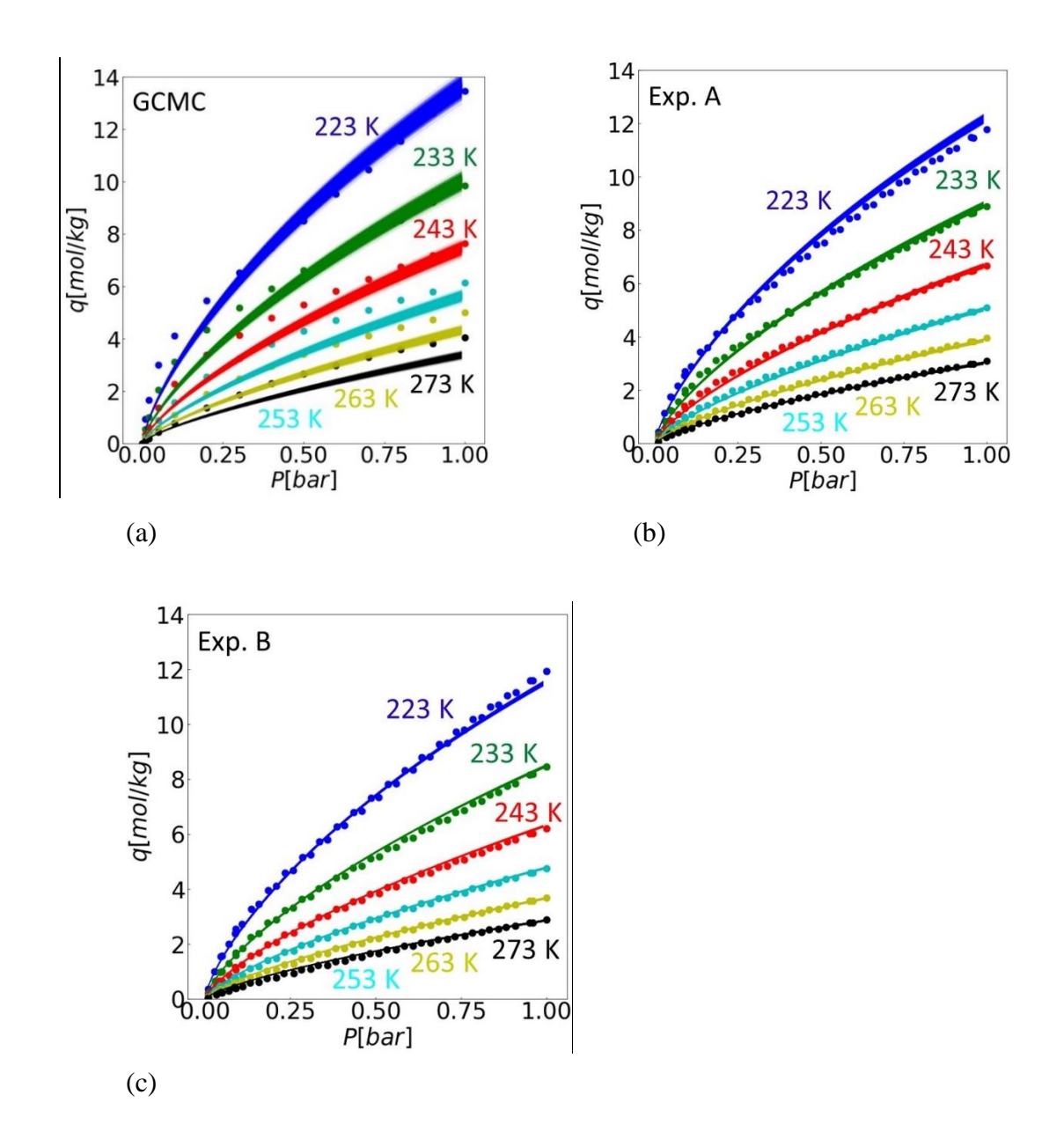


Figure 9 Data sets and the model plots using estimated isotherm parameters for MIL-101(Cr): (a) GCMC, (b) Exp. A, (c) Exp. B. The model plots are shown as lines using 5,000 points sampled from parameter posterior distributions.

Lastly, correlations for isotherm parameter pairs are evaluated for MIL-101(Cr) by pair plots shown in Figure 10. We find a weak correlation for n vs. $-\Delta H$ whereas relatively strong correlations can be found for for b_0 vs. $-\Delta H$ and b_0 vs. n. Since the mean of the posterior distribution of q_s reached the upper bound of the prior distribution, correlations of this parameter with other parameters cannot be analyzed.

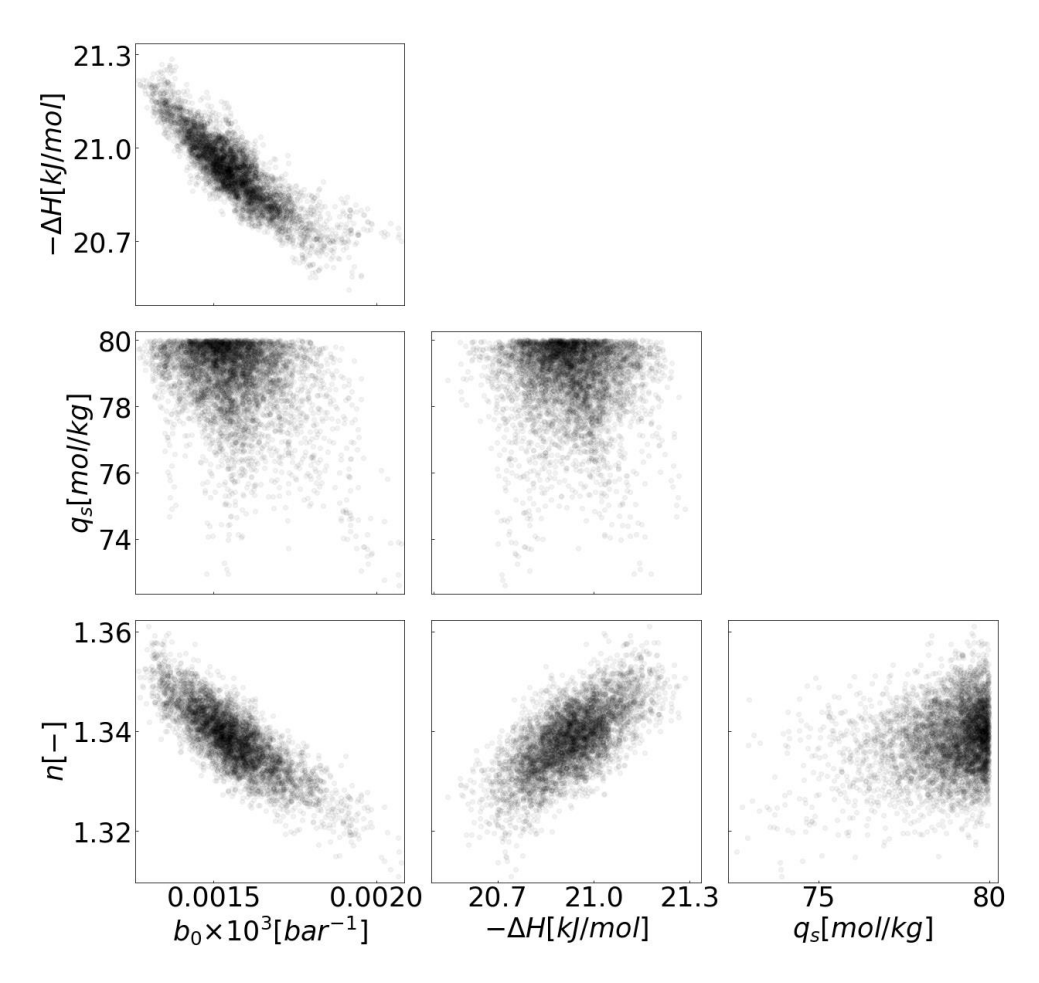


Figure 10 Parameter pair plots of adsorption isotherm model for MIL-101(Cr). In each pair plot, 5,000 points are sampled from parameter posterior distributions.

4. Conclusions

In this study, a hierarchical Bayesian estimation framework using the MCMC method was demonstrated to quantify the discrepancy between data sets of experimental measurements and GCMC simulation. As a case study, CO_2 adsorption isotherms in nanoporous adsorbents were considered. Multiple data sets for CO_2 adsorption isotherms onto zeolite 13X and MIL-101(Cr) at different conditions were used. The proposed framework estimated the parameters of adsorption isotherm models as probability distributions. At the same time, the discrepancy between the simulated and experimental data was quantified through probability distributions of the multiplicative coefficient R_i and variance of measurement errors σ_i .

The proposed approach was demonstrated successfully for the first case study of zeolite 13X. It was found that the posterior distributions of isotherm equation parameters

and hyperparameters were obtained as unimodal and symmetric distributions. Particularly, the identification of data sets that closely match with the GCMC data, as well as outlier data sets which deviate significantly from the reference GCMC data, enabled by the proposed R_i factor was achieved. We showed that introducing the coefficient R_i was effective to deal with disparate temperature ranges in the measurements. These results imply that our proposed approach can be a useful technique to analyze the quality of data. Although the underlying contributors for given data quality may not necessarily be identified, the proposed framework provides insights into analyzing inconsistencies that exist between a set of experimental data and molecular simulation.

The proposed framework was also demonstrated for another case study of MIL-101(Cr), identifying some remaining challenges due to the relatively limited adsorption data in this study. The prior distribution for one of the parameters in the Sips isotherm model chosen in this study always reached the upper bound of the prior distribution, which may be due to model inadequacy. Modification of the model and obtaining additional data sets over a wider temperature range may resolve this problem. Also R_i of our experimental attempts indicated the underestimation of the adsorbed amount measured experimentally compared to the reference GCMC data, which may be partly explained by the difference of computed and measured surface areas.

The proposed framework is an effective approach to quantify the discrepancies between adsorption isotherms measured experimentally and simulated, which is noted frequently in literature. Thorough understanding on these inconsistencies and, more importantly, providing the most probable isotherm parameters will be a vital input for process modeling not only in CO₂ capture but also in other application areas of adsorptive separation.

Declarations of Interest

None

Acknowledgments

This study was supported by the Japan Society for the Promotion of Science (JSPS) Grants-in-Aid for Scientific Research, Grant Number JP18H01776. DSS and KW acknowledge support from the Center for Understanding and Control of Acid Gas-Induced Evolution of Materials for Energy (UNCAGE-ME), an Energy Frontier Research Center funded by the U.S. Department of Energy, Office of Science, Office of Basic Energy Sciences, under Award No. DE-SC0012577.

Nomenclature

 A_t : temperature dependence constant of parameter t

 b_S : affinity constant in Sips model

 b_{S0} : affinity constant in Sips model

 b_T : Toth constant

 B_t : temperature dependence constant of parameter t

 b_{T0} : affinity constant

i: index of data set

n: Sips constant

p: partial pressure of CO_2

p(y): marginal likelihood

 $p(\theta, \phi | y)$: posterior distribution

 $p(y|\theta)$: likelihood representing the probability of data y at a given parameter θ

 $p(\mathbf{y}_i|\sigma_i)$: posterior distribution

 $p(\varphi)$: hyperprior distribution

 $p(\theta)$: prior probability distribution of θ

 $p(\theta|\mathbf{y})$: posterior distribution of the parameters

 q^* : equilibrium amount of CO₂ adsorbed

 q_s : saturated amount of CO₂ adsorbed

R: ideal gas constant

 R_i : measurement error for each data y_i

T: temperature

t: Toth constant representing heterogeneity of adsorption system

y: vector of data such as experimental results

 θ : parameter vector to be estimated

 ω : parameter vector of each data set representing individual unique properties

 φ : hyperparameter

 ΔH : isosteric heat of adsorption

 σ_i : standard deviation (SD) of vector y_i

Abbreviations

AIC: Akaike information criterion

BIC: Bayesian information criterion

CCUS: carbon capture, utilization, and storage

GCMC: grand canonical Monte Carlo

HPD: highest posterior density

HYBRID: hybrid fractional error function

MCMC: Markov chain Monte Carlo

MOF: metal organic framework

NIST: National Institute of Standards and Technology

RMSD: root mean square deviation

SD: standard deviation

SSE: sum of squares of errors

Reference

- [1] K. Adil, P. Bhatt, Y. Belmabkhout, S. M. T Abtab, H. Jiang, A. Assen, A. Mallick, A. Cadiau, J. Aqil, M. Eddaoudi, "Valuing Metal–Organic Frameworks for Postcombustion Carbon Capture: A Benchmark Study for Evaluating Physical Adsorbents," *Adv. Mater.*, vol. 29, no. 39, pp. 1–10, 2017, doi: 10.1002/adma.201702953.
- [2] I. Taniguchi, K. Kinugasa, M. Toyoda, K. Minezaki, H. Tanaka, and K. Mitsuhara, "Piperazine-immobilized polymeric membranes for CO₂ capture: mechanism of preferential CO₂ permeation," *Polym. J.*, vol. 53, no. 1, pp. 129–136, 2021, doi: 10.1038/s41428-020-0389-7.
- [3] X. Wang, Q. Guo, J. Zhao, and L. Chen, "Mixed amine-modified MCM-41 sorbents for CO₂ capture," *Int. J. Greenh. Gas Control*, vol. 37, pp. 90–98, 2015, doi: 10.1016/j.ijggc.2015.03.018.
- [4] R. H. K. Scott, R. Hughes, *Industrial Membrane Separation Technology*. Springer Science & Business Media, 1996.
- [5] D. Aaron and C. Tsouris, "Separation of CO₂ from flue gas: A review," Sep. Sci. Technol., vol. 40, no. 1–3, pp. 321–348, 2005, doi: 10.1081/SS-200042244.
- [6] K. T. Leperi, Y. G. Chung, F. You, and R. Q. Snurr, "Development of a General Evaluation Metric for Rapid Screening of Adsorbent Materials for Postcombustion CO₂ Capture," ACS Sustain. Chem. Eng., vol. 7, no. 13, pp. 11529–11539, 2019, doi: 10.1021/acssuschemeng.9b01418.
- [7] J. Park, H. O. Rubiera Landa, Y. Kawajiri, M. J. Realff, R. P. Lively, and D. S. Sholl, "How Well Do Approximate Models of Adsorption-Based CO₂ Capture Processes Predict Results of Detailed Process Models?," *Ind. Eng. Chem. Res.*, vol. 59, no. 15, pp. 7097–7108, 2020, doi: 10.1021/acs.iecr.9b05363.
- [8] Siderius, D.W. and Shen, V.K., Eds., "NIST adsorption." [Online], The NIST Registry of Adsorbent Materials, National Institute of Standards and Technology, Gaithersburg MD, 20899, https://dx.doi.org/10.18434/t4/1502644, (retrieved October 11, 2021)..
- [9] J. Park, J. D. Howe, and D. S. Sholl, "How Reproducible Are Isotherm Measurements in Metal-Organic Frameworks?," *Chem. Mater.*, vol. 29, no. 24, pp. 10487–10495, 2017, doi: 10.1021/acs.chemmater.7b04287.
- [10] L. W. Bingel, A. Chen, M. Agrawal, and D. S. Sholl, "Experimentally Verified Alcohol Adsorption Isotherms in Nanoporous Materials from Literature Meta-Analysis," *J. Chem. Eng. Data*, vol. 65, no. 10, pp. 4970–4979, 2020, doi: 10.1021/acs.jced.0c00598.
- [11] X. Cai, F. Gharagheizi, L. W. Bingel, D. Shade, K. S. Walton, and D. S. Sholl, "A Collection of More than 900 Gas Mixture Adsorption Experiments in Porous Materials from Literature Meta-Analysis," *Ind. Eng. Chem. Res.*, vol. 60, no. 1, pp. 639–651, 2021, doi: 10.1021/acs.iecr.0c05398.
- [12] W. Franus, M. Wdowin, and M. Franus, "Synthesis and characterization of zeolites prepared from

- industrial fly ash," *Environ. Monit. Assess.*, vol. 186, no. 9, pp. 5721–5729, 2014, doi: 10.1007/s10661-014-3815-5.
- [13] N. C. Burtch, H. Jasuja, and K. S. Walton, "Water stability and adsorption in metal-organic frameworks," *Chem. Rev.*, vol. 114, no. 20, pp. 10575–10612, 2014, doi: 10.1021/cr5002589.
- [14] S. Bourrelly, P. L. Llewellyn, C. Serre, F. Millange, T. Loiseau, and G. Férey, "Different adsorption behaviors of methane and carbon dioxide in the isotypic nanoporous metal terephthalates MIL-53 and MIL-47," *J. Am. Chem. Soc.*, vol. 127, no. 39, pp. 13519–13521, 2005, doi: 10.1021/ja054668v.
- [15] B. Arstad, H. Fjellvåg, K. O. Kongshaug, O. Swang, and R. Blom, "Amine functionalised metal organic frameworks (MOFs) as adsorbents for carbon dioxide," *Adsorption*, vol. 14, no. 6, pp. 755–762, 2008, doi: 10.1007/s10450-008-9137-6.
- [16] D. S. Sholl and R. P. Lively, "Defects in Metal-Organic Frameworks: Challenge or Opportunity?," *J. Phys. Chem. Lett.*, vol. 6, no. 17, pp. 3437–3444, 2015, doi: 10.1021/acs.jpclett.5b01135.
- [17] T. Düren, Y. S. Bae, and R. Q. Snurr, "Using molecular simulation to characterise metal-organic frameworks for adsorption applications," *Chem. Soc. Rev.*, vol. 38, no. 5, pp. 1237–1247, 2009, doi: 10.1039/b803498m.
- [18] S. Keskin, J. Liu, R. B. Rankin, J. K. Johnson, and D. S. Sholl, "Progress, opportunities, and challenges for applying atomically detailed modeling to molecular adsorption and transport in metal Organic framework materials," *Ind. Eng. Chem. Res.*, vol. 48, no. 5, pp. 2355–2371, 2009, doi: 10.1021/ie800666s.
- [19] F. X. Coudert and A. H. Fuchs, "Computational characterization and prediction of metal-organic framework properties," *Coord. Chem. Rev.*, vol. 307, pp. 211–236, 2016, doi: 10.1016/j.ccr.2015.08.001.
- [20] M. Witman, S. Ling, S. Jawahery, P. G. Boyd, M. Haranczyk, B. Slater, B. Smit, "The Influence of Intrinsic Framework Flexibility on Adsorption in Nanoporous Materials," *J. Am. Chem. Soc.*, vol. 139, no. 15, pp. 5547–5557, 2017, doi: 10.1021/jacs.7b01688.
- [21] J. Park, M. Agrawal, D. F. Sava Gallis, J. A. Harvey, J. A. Greathouse, and D. S. Sholl, "Impact of intrinsic framework flexibility for selective adsorption of sarin in non-aqueous solvents using metal-organic frameworks," *Phys. Chem. Chem. Phys.*, vol. 22, no. 11, pp. 6441–6448, 2020, doi: 10.1039/c9cp06788d.
- [22] H. Fang, H. Demir, P. Kamakoti, and D. S. Sholl, "Recent developments in first-principles force fields for molecules in nanoporous materials," *J. Mater. Chem. A*, vol. 2, no. 2, pp. 274–291, 2014, doi: 10.1039/c3ta13073h.
- [23] J. Kim, L. C. Lin, K. Lee, J. B. Neaton, and B. Smit, "Efficient determination of accurate force fields for porous materials using ab initio total energy calculations," *J. Phys. Chem. C*, vol. 118,

- no. 5, pp. 2693–2701, 2014, doi: 10.1021/jp412368m.
- [24] C. Shih, J. Park, D. S. Sholl, M. J. Realff, T. Yajima, and Y. Kawajiri, "Hierarchical Bayesian estimation for adsorption isotherm parameter determination," *Chem. Eng. Sci.*, vol. 214, pp. 1–21, 2020, doi: 10.1016/j.ces.2019.115435.
- [25] D. B. R. Andrew Gelman, John B. Carlin, Hal S. Stern, *Bayesian Data Analysis*, Second Edi. Chapman & Hall/CRC Texts in Statistical Science, 2003.
- [26] B. Smit, "Grand canonical monte carlo simulations of chain molecules: Adsorption isotherms of alkanes in zeolites," *Mol. Phys.*, vol. 85, no. 1, pp. 153–172, 1995, doi: 10.1080/00268979500101011.
- [27] L. Joos, J. A. Swisher, and B. Smit, "Molecular simulation study of the competitive adsorption of H₂O and CO₂ in zeolite 13X," *Langmuir*, vol. 29, no. 51, pp. 15936–15942, 2013, doi: 10.1021/la403824g.
- [28] R. Krishna and J. M. van Baten, "Segregation effects in adsorption of CO₂-containing mixtures and their consequences for separation selectivities in cage-type zeolites," *Sep. Purif. Technol.*, vol. 61, no. 3, pp. 414–423, 2008, doi: 10.1016/j.seppur.2007.12.003.
- [29] S. Keskin, T. M. van Heest, and D. S. Sholl, "Can metal-organic framework materials play a useful role in large-scale carbon dioxide separations?," *ChemSusChem*, vol. 3, no. 8, pp. 879–891, 2010, doi: 10.1002/cssc.201000114.
- [30] D. Bonenfant, M. Kharoune, P. Niquette, M. Mimeault, and R. Hausler, "Advances in principal factors influencing carbon dioxide adsorption on zeolites," *Sci. Technol. Adv. Mater.*, vol. 9, no. 1, 2008, doi: 10.1088/1468-6996/9/1/013007.
- [31] H. G. T. Nguyen, L. Espinal, R. D. van Zee, M. Thommes, B. Toman, M. S. L. Hudson, E. Mangano, S. Brandani, D. P. Broom, M. J. Benham, K. Cychosz, P. Bertier, F. Yang, B. M. Krooss, R. L. Siegelman, M. Hakuman, K. Nakai, A. D. Ebner, L. Erden, J. A. Ritter, A. Moran, O. Talu, Y. Huang, K. S. Walton, P. Billemont, G. De Weireld, "A reference high-pressure CO₂ adsorption isotherm for ammonium ZSM-5 zeolite: results of an interlaboratory study," *Adsorption*, vol. 24, no. 6, pp. 531–539, 2018, doi: 10.1007/s10450-018-9958-x.
- [32] Z. Zhao, X. Cui, J. Ma, and R. Li, "Adsorption of carbon dioxide on alkali-modified zeolite 13X adsorbents," *Int. J. Greenh. Gas Control*, vol. 1, no. 3, pp. 355–359, 2007, doi: 10.1016/S1750-5836(07)00072-2.
- [33] Z. Zhang, W. Zhang, X. Chen, Q. Xia, and Z. Li, "Adsorption of CO₂ on zeolite 13X and activated carbon with higher surface area," *Sep. Sci. Technol.*, vol. 45, no. 5, pp. 710–719, 2010, doi: 10.1080/01496390903571192.
- [34] X. Peng, W. Wang, R. Xue, and Z. Shen, "Adsorption separation of CH₄/CO₂ on mesocarbon microbeads: Experiment and modeling," *AIChE J.*, vol. 52, no. 3, pp. 994–1003, 2006, doi: 10.1002/aic.10723.

- [35] G. Li, P. Xiao, P. Webley, J. Zhang, R. Singh, and M. Marshall, "Capture of CO₂ from high humidity flue gas by vacuum swing adsorption with zeolite 13X," *Adsorption*, vol. 14, no. 2–3, pp. 415–422, 2008, doi: 10.1007/s10450-007-9100-y.
- [36] J. Zhang, P. Xiao, G. Li, and P. A. Webley, "Effect of flue gas impurities on CO₂ capture performance from flue gas at coal-fired power stations by vacuum swing adsorption," *Energy Procedia*, vol. 1, no. 1, pp. 1115–1122, 2009, doi: 10.1016/j.egypro.2009.01.147.
- [37] D. Luebke, C. Myers, and H. Pennline, "Hybrid membranes for selective carbon dioxide separation from fuel gas," *Energy and Fuels*, vol. 20, no. 5, pp. 1906–1913, 2006, doi: 10.1021/ef060060b.
- [38] Y. Lin, C. Kong, and L. Chen, "Direct synthesis of amine-functionalized MIL-101(Cr) nanoparticles and application for CO₂ capture," *RSC Adv.*, vol. 2, no. 16, pp. 6417–6419, 2012, doi: 10.1039/c2ra20641b.
- [39] C. Férey, C. Mellot-Draznieks, C. Serre, F. Millange, J. Dutour, S. Surblé, I. Margiolaki, "Chemistry: A chromium terephthalate-based solid with unusually large pore volumes and surface area," *Science* (80-.)., vol. 309, no. 5743, pp. 2040–2042, 2005, doi: 10.1126/science.1116275.
- [40] Q. Liu, L. Ning, S. Zheng, M. Tao, Y. Shi, and Y. He, "Adsorption of Carbon Dioxide by MIL-101(Cr): Regeneration conditions and influence of flue gas contaminants," *Sci. Rep.*, vol. 3, pp. 1–6, 2013, doi: 10.1038/srep02916.
- [41] S. J. A. DeWittt, R. Awati, H. Octavio Rubiera Landa, J. Park, Y. Kawajiri, D. S. Sholl, M. J. Realff, R. P. Lively, "Analysis of energetics and economics of sub-ambient hybrid post-combustion carbon dioxide capture," *AIChE J.*, no. June, pp. 1–14, 2021, doi: 10.1002/aic.17403.
- [42] Z. Bao, L. Yu, Q. Ren, X. Lu, and S. Deng, "Adsorption of CO₂ and CH₄ on a magnesium-based metal organic framework," *J. Colloid Interface Sci.*, vol. 353, no. 2, pp. 549–556, 2011, doi: 10.1016/j.jcis.2010.09.065.
- [43] H. Deng, H. Yi, X. Tang, Q. Yu, P. Ning, and L. Yang, "Adsorption equilibrium for sulfur dioxide, nitric oxide, carbon dioxide, nitrogen on 13X and 5A zeolites," *Chem. Eng. J.*, vol. 188, pp. 77–85, 2012, doi: 10.1016/j.cej.2012.02.026.
- [44] Y. Wang and M. D. LeVan, "Adsorption equilibrium of carbon dioxide and water vapor on zeolites 5a and 13X and silica gel: Pure components," *J. Chem. Eng. Data*, vol. 54, no. 10, pp. 2839–2844, 2009, doi: 10.1021/je800900a.
- [45] S. Cavenati, C. A. Grande, and A. E. Rodrigues, "Adsorption Equilibrium of Methane, Carbon Dioxide, and Nitrogen on Zeolite 13X at High Pressures," *J. Chem. Eng. Data*, vol. 49, no. 4, pp. 1095–1101, 2004, doi: 10.1021/je0498917.
- [46] J. A. C. Silva, K. Schumann, and A. E. Rodrigues, "Sorption and kinetics of CO₂ and CH₄ in binderless beads of 13X zeolite," *Microporous Mesoporous Mater.*, vol. 158, pp. 219–228, 2012,

- doi: 10.1016/j.micromeso.2012.03.042.
- [47] M. J. Purdue and Z. Qiao, "Molecular simulation study of wet flue gas adsorption on zeolite 13X," *Microporous Mesoporous Mater.*, vol. 261, no. October 2017, pp. 181–197, 2018, doi: 10.1016/j.micromeso.2017.10.059.
- [48] H. Fang, J. Findley, G. Muraro, P. I. Ravikovitch, and D. S. Sholl, "A Strong Test of Atomically Detailed Models of Molecular Adsorption in Zeolites Using Multilaboratory Experimental Data for CO2 Adsorption in Ammonium ZSM-5," *J. Phys. Chem. Lett.*, vol. 11, no. 2, pp. 471–477, 2020, doi: 10.1021/acs.jpclett.9b02986.
- [49] J. Park, R. P. Lively, and D. S. Sholl, "Establishing upper bounds on CO₂ swing capacity in sub-ambient pressure swing adsorption via molecular simulation of metal-organic frameworks," *J. Mater. Chem. A*, vol. 5, no. 24, pp. 12258–12265, 2017, doi: 10.1039/c7ta02916k.
- [50] D. Dubbeldam, A. Torres-Knoop, and K. S. Walton, "On the inner workings of monte carlo codes," *Molecular Simulation*, vol. 39, no. 14–15. Taylor & Francis, pp. 1253–1292, 2013, doi: 10.1080/08927022.2013.819102.
- [51] D. Dubbeldam, S. Calero, D. E. Ellis, and R. Q. Snurr, "RASPA: Molecular simulation software for adsorption and diffusion in flexible nanoporous materials," *Mol. Simul.*, vol. 42, no. 2, pp. 81– 101, 2016, doi: 10.1080/08927022.2015.1010082.
- [52] A. K. Rappé, C. J. Casewit, K. S. Colwell, W. A. Goddard, and W. M. Skiff, "UFF, a Full Periodic Table Force Field for Molecular Mechanics and Molecular Dynamics Simulations," *J. Am. Chem. Soc.*, vol. 114, no. 25, pp. 10024–10035, 1992, doi: 10.1021/ja00051a040.
- [53] K. A. Maerzke and J. I. Siepmann, "Transferable potentials for phase equilibria Coarse-Grain description for linear alkanes," *J. Phys. Chem. B*, vol. 115, no. 13, pp. 3452–3465, 2011, doi: 10.1021/jp1063935.
- [54] T. D. Allen MP, Computer Simulation of Liquids, Second. Oxford University Press, 1987.
- [55] B. A. Wells and A. L. Chaffee, "Ewald Summation for Molecular Simulations," *J. Chem. Theory Comput.*, vol. 11, no. 8, pp. 3684–3695, 2015, doi: 10.1021/acs.jctc.5b00093.
- [56] T. A. Manz and D. S. Sholl, "the Electrostatic Potential in Periodic and Nonperiodic Materials," *J. Chem. Theor. Comput.*, vol. 6, pp. 2455–2468, 2010.
- [57] T. A. Manz and D. S. Sholl, "Improved atoms-in-molecule charge partitioning functional for simultaneously reproducing the electrostatic potential and chemical states in periodic and nonperiodic materials," *J. Chem. Theory Comput.*, vol. 8, no. 8, pp. 2844–2867, 2012, doi: 10.1021/ct3002199.
- [58] T. Watanabe, T. A. Manz, and D. S. Sholl, "Accurate treatment of electrostatics during molecular adsorption in nanoporous crystals without assigning point charges to framework atoms," *J. Phys. Chem. C*, vol. 115, no. 11, pp. 4824–4836, 2011, doi: 10.1021/jp201075u.
- [59] L. A. Darunte, A. D. Oetomo, K. S. Walton, D. S. Sholl, and C. W. Jones, "Direct Air Capture of

- CO₂ Using Amine Functionalized MIL-101(Cr)," *ACS Sustain. Chem. Eng.*, vol. 4, no. 10, pp. 5761–5768, 2016, doi: 10.1021/acssuschemeng.6b01692.
- [60] Y. Park, D. K. Moon, Y. H. Kim, H. Ahn, and C. H. Lee, "Adsorption isotherms of CO₂, CO, N₂, CH₄, Ar and H₂ on activated carbon and zeolite LiX up to 1.0 MPa," *Adsorption*, vol. 20, no. 4, pp. 631–647, 2014, doi: 10.1007/s10450-014-9608-x.
- [61] A. I. Sarker, A. Aroonwilas, and A. Veawab, "Equilibrium and Kinetic Behaviour of CO₂
 Adsorption onto Zeolites, Carbon Molecular Sieve and Activated Carbons," *Energy Procedia*, vol. 114, no. November 2016, pp. 2450–2459, 2017, doi: 10.1016/j.egypro.2017.03.1394.
- [62] O. M. Akpa and E. I. Unuabonah, "Small-Sample Corrected Akaike Information Criterion: An appropriate statistical tool for ranking of adsorption isotherm models," *Desalination*, vol. 272, no. 1–3, pp. 20–26, 2011, doi: 10.1016/j.desal.2010.12.057.
- [63] M. M. Rahman, M. Muttakin, A. Pal, A. Z. Shafiullah, and B. B. Saha, "A statistical approach to determine optimal models for IUPAC-classified adsorption isotherms," *Energies*, vol. 12, no. 23, 2019, doi: 10.3390/en12234565.
- [64] M. M. Rahman, A. Pal, K. Uddin, K. Thu, and B. B. Saha, "Statistical analysis of optimized isotherm model for maxsorb III/ethanol and silica gel/water pairs," *Evergreen*, vol. 5, no. 4, pp. 1–12, 2018, doi: 10.5109/2174852.
- [65] G. F. Malash and M. I. El-Khaiary, "Methylene blue adsorption by the waste of Abu-Tartour phosphate rock," *J. Colloid Interface Sci.*, vol. 348, no. 2, pp. 537–545, 2010, doi: 10.1016/j.jcis.2010.05.005.
- [66] K. Zabielska, T. Aleksandrzak, and E. Gabruś, "Adsorption equilibrium of carbon dioxide on zeolite 13X at high pressures," *Chem. Process Eng. - Inz. Chem. i Proces.*, vol. 39, no. 3, pp. 309–321, 2018, doi: 10.24425/122952.
- [67] M. C. Campo, A. M. Ribeiro, A. Ferreira, J. C. Santos, C. Lutz, J. M. Loureiro, A. E. Rodrigues, "New 13X zeolite for propylene/propane separation by vacuum swing adsorption," *Sep. Purif. Technol.*, vol. 103, pp. 60–70, 2013, doi: 10.1016/j.seppur.2012.10.009.
- [68] Z. Qiao, Z. Wang, C. Zhang, S. Yuan, Y. Zhu, and J. Wang, "PVAm–PIP/PS composite membrane with high performance for CO₂/N₂ separation," *AIChE J.*, vol. 59, no. 4, pp. 215–228, 2012, doi: 10.1002/aic.
- [69] N. S. Wilkins, J. A. Sawada, and A. Rajendran, "Measurement of competitive CO₂ and H₂O adsorption on zeolite 13X for post-combustion CO₂ capture," *Adsorption*, vol. 26, no. 5, pp. 765–779, 2020, doi: 10.1007/s10450-020-00199-3.
- [70] P. Xiao, J. Zhang, P. Webley, G. Li, R. Singh, and R. Todd, "Capture of CO₂ from flue gas streams with zeolite 13X by vacuum-pressure swing adsorption," *Adsorption*, vol. 14, no. 4–5, pp. 575–582, 2008, doi: 10.1007/s10450-008-9128-7.
- [71] V. Garshasbi, M. Jahangiri, and M. Anbia, "Equilibrium CO₂ adsorption on zeolite 13X prepared

- from natural clays," *Appl. Surf. Sci.*, vol. 393, pp. 225–233, 2017, doi: 10.1016/j.apsusc.2016.09.161.
- [72] S. H. Hsu, S. D. Stamatis, J. M. Caruthers, W. N. Delgass, V. Venkatasubramanian, G. E. Blau, M. Lasinski, S. Orcun, "Bayesian framework for building kinetic models of catalytic systems," *Ind. Eng. Chem. Res.*, vol. 48, no. 10, pp. 4768–4790, 2009, doi: 10.1021/ie801651y.
- [73] F. Yuanhang, S. Dongli, Y. Zidong, L. Li, D. Jihui, and H. Wei, "Hierarchical Bayesian models for predicting soil salinity and sodicity characteristics in a coastal reclamation region," *Ecol. Eng.*, vol. 104, pp. 45–56, 2017, doi: 10.1016/j.ecoleng.2017.04.006.
- [74] A. J. Howarth, A. W. Peters, N. A. Vermeulen, T. C. Wang, J. T. Hupp, and O. K. Farha, "Best practices for the synthesis, activation, and characterization of metal–organic frameworks," *Chem. Mater.*, vol. 29, no. 1, pp. 26–39, 2017, doi: 10.1021/acs.chemmater.6b02626.
- [75] K. N. Son, G. E. Cmarik, J. C. Knox, J. A. Weibel, and S. V. Garimella, "Measurement and Prediction of the Heat of Adsorption and Equilibrium Concentration of CO₂ on Zeolite 13X," *J. Chem. Eng. Data*, vol. 63, no. 5, pp. 1663–1674, 2018, doi: 10.1021/acs.jced.8b00019.
- [76] Y. Belmabkhout, M. Frère, and G. De Weireld, "High-pressure adsorption measurements. A comparative study of the volumetric and gravimetric methods," *Meas. Sci. Technol.*, vol. 15, no. 5, pp. 848–858, 2004, doi: 10.1088/0957-0233/15/5/010.
- [77] K. G. Wynnyk, B. Hojjati, P. Pirzadeh, and R. A. Marriott, "High-pressure sour gas adsorption on zeolite 4A," *Adsorption*, vol. 23, no. 1, pp. 149–162, 2017, doi: 10.1007/s10450-016-9841-6.
- [78] J. Kalyanaraman, Y. Kawajiri, and M. J. Realff, "Bayesian design of experiments for adsorption isotherm modeling," *Comput. Chem. Eng.*, vol. 135, 2020, doi: 10.1016/j.compchemeng.2020.106774.
- [79] S. Angus, K. M. de Reuck, and B. Armstrong (1972) International Thermodynamic Tables of the Fluid-State 3, Carbon Dioxide, Pergamon Press, Oxford.
- [80] H. Demir, J. A. Greathouse, C. L. Staiger, J. J. Perry, M. D. Allendorf, and D. S. Sholl, "DFT-based force field development for noble gas adsorption in metal organic frameworks," *J. Mater. Chem. A*, vol. 3, no. 46, pp. 23539–23548, 2015, doi: 10.1039/c5ta06201b.
- [81] D. Dubbeldam, H. Frost, K. S. Walton, and R. Q. Snurr, "Molecular simulation of adsorption sites of light gases in the metal-organic framework IRMOF-1," *Fluid Phase Equilib.*, vol. 261, no. 1–2, pp. 152–161, 2007, doi: 10.1016/j.fluid.2007.07.042.
- [82] S. Surblé, F. Millange, C. Serre, T. Düren, M. Latroche, S. Bourrelly, P. L. Llewellyn, G. Férey, "Synthesis of MIL-102, a chromium carboxylate metal-organic framework, with gas sorption analysis," *J. Am. Chem. Soc.*, vol. 128, no. 46, pp. 14889–14896, 2006, doi: 10.1021/ja064343u.
- [83] J. G. McDaniel, S. Li, E. Tylianakis, R. Q. Snurr, and J. R. Schmidt, "Evaluation of force field performance for high-throughput screening of gas uptake in metal-organic frameworks," *J. Phys. Chem. C*, vol. 119, no. 6, pp. 3143–3152, 2015, doi: 10.1021/jp511674w.

- [84] J. R. Schmidt, K. Yu, and J. G. McDaniel, "Transferable Next-Generation Force Fields from Simple Liquids to Complex Materials," Acc. Chem. Res., vol. 48, no. 3, pp. 548–556, 2015, doi: 10.1021/ar500272n.
- [85] R. Mercado, B. Vlaisavljevich, L. C. Lin, K. Lee, Y. Lee, J. A. Mason, D. J. Xiao, M. I. Gonzalez, M. T. Kapelewski, J. B. Neaton, B. Smit, "Force Field Development from Periodic Density Functional Theory Calculations for Gas Separation Applications Using Metal-Organic Frameworks," J. Phys. Chem. C, vol. 120, no. 23, pp. 12590–12604, 2016, doi: 10.1021/acs.jpcc.6b03393.

Conflict of Interest

Declaration of interests

⊠The authors declare that they have no known competing financial interests or personal relationships
that could have appeared to influence the work reported in this paper.
□The authors declare the following financial interests/personal relationships which may be considered
as potential competing interests: